

Gap function and density of states in the strong-coupling limit for an electron-boson system

F. Marsiglio*

*Department of Physics, University of California, San Diego, La Jolla, California 92093
and Physics Department, McMaster University, Hamilton, Ontario, Canada L8S 4M1*

J. P. Carbotte

Physics Department, McMaster University, Hamilton, Ontario, Canada L8S 4M1

(Received 10 September 1990)

We have calculated the frequency-dependent gap function for a superconductor in the strong-coupling limit $\lambda \gg 1$, where λ is the electron-boson mass-renormalization parameter. We find a multip peaked function which leads to a spectral function with quasiparticle-like resonances on an energy scale determined by the gap. This is in contrast to the moderate-coupling regime, $\lambda \approx 1$, where structure occurs on an energy scale determined by the boson frequency.

I. INTRODUCTION

The observation of superconductivity at elevated temperatures¹ has led to intense theoretical activity in this field. There is certainly no consensus as to the mechanism responsible, although there is now substantial evidence that an *s*-wave BCS-like ground state is appropriate.²

One possibility that has received some attention³⁻⁹ is the asymptotic limit of Eliashberg theory with the arbitrary kernel applicable to any boson exchange mechanism, with phonons only one of the possibilities. In previous work the asymptotic behavior of T_c has been considered,¹⁰ as well as the gap ratio, $2\Delta_0/k_B T_c$,³⁻⁷ and the thermodynamics, critical magnetic fields, and penetration depths.^{4,5,8} In this paper we calculate the frequency dependence of the gap function $\Delta(\omega)$ and renormalization function $Z(\omega)$, from which the spectral function and quasiparticle density of states follow. We utilize the imaginary-axis formulation,¹¹⁻¹³ along with the exact analytic continuation equations derived in Ref. 14. In Sec. II we review the formalism. In Sec. III we show some results for large λ , and in Sec. IV we present results in the asymptotic limit ($\lambda \rightarrow \infty$). A brief summary is given in Sec. V.

II. FORMALISM

In order to simplify our results we use a boson spectral function represented by a single Einstein harmonic oscillator, with weight A at frequency ν_E . The limit $\lambda \rightarrow \infty$ can be achieved in several ways; here, we keep the area A fixed and allow $\nu_E \rightarrow 0$ ($\lambda \equiv 2A/\nu_E$). The Eliashberg equations on the imaginary axis are as follows:¹²

$$Z(i\omega_n)\Delta(i\omega_n) = \pi T \sum_{m=-\infty}^{\infty} \lambda(i\omega_m - i\omega_n) \frac{\Delta(i\omega_m)}{[\omega_m^2 + \Delta^2(i\omega_m)]^{1/2}}, \quad (1a)$$

$$Z(i\omega_n)$$

$$= 1 + \frac{\pi T}{\omega_n} \sum_{m=-\infty}^{\infty} \lambda(i\omega_m - i\omega_n) \frac{\omega_m}{[\omega_m^2 + \Delta^2(i\omega_m)]^{1/2}}, \quad (1b)$$

where $i\omega_n \equiv i\pi T(2n - 1)$, $n = 0, \pm 1, \pm 2, \dots$ are the fermion Matsubara frequencies and $Z(i\omega_n)$ and $\Delta(i\omega_n)$ are the renormalization and gap functions, respectively. The weighted boson propagator $\lambda(z)$ is given by

$$\lambda(z) = \frac{2Av_E}{v_E^2 - z^2}, \quad (2)$$

where we have used $\alpha^2 F(\nu) \equiv A\delta(\nu - \nu_E)$. Equations (1) are easily solved for any set of parameters, A , ν_E , and temperature, T . It is worthwhile noting that at $T=0$, Eqs. (1) become integral equations. In practice, one can solve these equations at some low reduced temperature, $t \equiv T/T_c \approx 0.1$ which for all practical purposes gives the "zero-temperature" solution. This is possible due to the existence of a gap at zero temperature in the excitation spectrum. However, one should note that depending on the values of A and ν_E , the "zero-temperature" solution sometimes occurs only for much lower values of reduced temperature, for example, $t \approx 0.01$, as we shall see below.

In Eqs. (1), $\lambda(0)$ cancels. Because of this, one can scale the gap function and temperature, to obtain the asymptotic gap equation, when $\nu_E \rightarrow 0$ ($\lambda \rightarrow \infty$):³

$$\bar{\Delta}(i\bar{\omega}_n) = 2\pi\bar{T} \sum_{m \neq n} \frac{1}{[2\pi\bar{T}(m - n)]^2} \frac{\bar{\Delta}(i\bar{\omega}_m) - \frac{\bar{\omega}_m}{\bar{\omega}_n} \bar{\Delta}(i\bar{\omega}_n)}{[\bar{\omega}_m^2 + \bar{\Delta}^2(i\bar{\omega}_m)]^{1/2}}, \quad (3)$$

where $\bar{Q} \equiv Q / Av_E$, for any Q in Eq. (3). Equation (3) is universal, and independent of material parameters. The tacit assumption in the derivation of Eq. (3) is that $2\pi T \gg v_E$ or $\sqrt{\lambda}t \gg 1$, which can always be satisfied for finite t (since $v_E \rightarrow 0$). What is not obvious, and has only been verified numerically, is that "zero-temperature" behavior can be achieved with nonzero t , so that the conditions are satisfied. Once the gap and renormalization functions have been computed on the imaginary axis, an

analytic continuation to the real axis is required. Previously, one either solved the real-axis equations themselves,¹⁵ or used Padé approximates.¹⁶ The former method is time consuming and formidable in the regime we wish to investigate, and the latter is untested in the very-strong-coupling regime ($\lambda \rightarrow \infty$). We have used the equations recently derived in Ref. 14, which can be easily solved numerically. These are

$$Z(z)\Delta(z) = \pi T \sum_{m=-\infty}^{\infty} \lambda(z - i\omega_m) \frac{\Delta(i\omega_m)}{[\omega_m^2 + \Delta^2(i\omega_m)]^{1/2}} + i\pi A \left[[N(v_E) + f(v_E - z)] \frac{\Delta(z - v_E)}{[(z - v_E)^2 - \Delta^2(z - v_E)]^{1/2}} + [N(v_E) + f(v_E + z)] \frac{\Delta(z + v_E)}{[(z + v_E)^2 - \Delta^2(z + v_E)]^{1/2}} \right], \quad (4a)$$

$$Z(z) = 1 + \frac{i\pi T}{z} \sum_{m=-\infty}^{\infty} \lambda(z - i\omega_m) \frac{\omega_m}{[\omega_m^2 + \Delta^2(i\omega_m)]^{1/2}} + \frac{i\pi A}{z} \left[[N(v_E) + f(v_E - z)] \frac{z - v_E}{[(z - v_E)^2 - \Delta^2(z - v_E)]^{1/2}} + [N(v_E) + f(v_E + z)] \frac{z + v_E}{[(z + v_E)^2 - \Delta^2(z + v_E)]^{1/2}} \right]. \quad (4b)$$

Here, $z \equiv \omega + i\delta$, and $N(v_E)$ and $f(x)$ are the Bose and Fermi functions, respectively. Note that Eqs. (4) give the correct analytic continuation in the upper half plane [there are obviously correction terms beyond just replacing the " $i\omega_n$ " in Eqs. (1) by " z "].

In the asymptotic limit, Eqs. (4) become

$$Z(\bar{\omega})\bar{\Delta}(\bar{\omega}) = 2\pi\bar{T} \sum_{m=-\infty}^{\infty} \frac{\bar{\omega}_m^2 - \bar{\omega}^2}{(\bar{\omega}_m^2 + \bar{\omega}^2)^2} \frac{\bar{\Delta}(i\bar{\omega}_m)}{[\bar{\omega}_m^2 + \bar{\Delta}^2(i\bar{\omega}_m)]^{1/2}} + \lim_{\bar{v}_E \rightarrow 0} \left[\frac{i\pi}{\bar{v}_E} \right] \left[[N(\bar{v}_E) + f(\bar{v}_E - \bar{\omega})] \frac{\bar{\Delta}(\bar{\omega} - \bar{v}_E)}{[(\bar{\omega} - \bar{v}_E)^2 - \bar{\Delta}^2(\bar{\omega} - \bar{v}_E)]^{1/2}} + [N(\bar{v}_E) + f(\bar{v}_E + \bar{\omega})] \frac{\bar{\Delta}(\bar{\omega} + \bar{v}_E)}{[(\bar{\omega} + \bar{v}_E)^2 - \bar{\Delta}^2(\bar{\omega} + \bar{v}_E)]^{1/2}} \right], \quad (5a)$$

$$Z(\bar{\omega}) = 1 + 4\pi\bar{T} \sum_{m=-\infty}^{\infty} \frac{1}{(\bar{\omega}_m^2 + \bar{\omega}^2)^2} \frac{\bar{\omega}_m^2}{[\bar{\omega}_m^2 + \bar{\Delta}^2(i\bar{\omega}_m)]^{1/2}} + \lim_{\bar{v}_E \rightarrow 0} \left[\frac{i\pi}{\bar{v}_E\bar{\omega}} \right] \left[[N(\bar{v}_E) + f(\bar{v}_E - \bar{\omega})] \frac{\bar{\omega} - \bar{v}_E}{[(\bar{\omega} - \bar{v}_E)^2 - \bar{\Delta}^2(\bar{\omega} - \bar{v}_E)]^{1/2}} + [N(\bar{v}_E) + f(\bar{v}_E + \bar{\omega})] \frac{\bar{\omega} + \bar{v}_E}{[(\bar{\omega} + \bar{v}_E)^2 - \bar{\Delta}^2(\bar{\omega} + \bar{v}_E)]^{1/2}} \right]. \quad (5b)$$

Equations (5) do not obey straightforward scaling relations. Furthermore, the limiting behavior $\bar{v}_E \rightarrow 0$ occurs in a quite different manner depending on whether we take $T=0$ or $T>0$. For $T>0$, $N(\bar{v}_E) \sim \bar{T}/\bar{v}_E$ and $f(\bar{v}_E \pm \bar{\omega}) \sim f(\pm \bar{\omega})$. Singular terms cancel when Eqs. (5a) and (5b) are combined. The result is a second-order differential equation in the scaled variables with no material-dependent parameters present. Then, the gap edge scales according to $\Delta_0/\sqrt{Av_E} \sim c$, where c is some number. Coupled with the Allen-Dynes result, that $T_c = 0.2584\sqrt{Av_E}$, we find $2\Delta_0/k_B T_c = \text{const}$, in the limit $\lambda \rightarrow \infty$, as proven in Ref. 2 (the claim that $2\Delta_0/k_B T_c \propto \sqrt{\lambda}$ given in Ref. 4 is, in our opinion, incorrect). For $T=0$, $N(\bar{v}_E) \equiv 0$, and $f(\bar{v}_E \pm \bar{\omega}) = \Theta(\pm \bar{\omega} - \bar{v}_E)$, the unit step function. Again, combining Eqs. (5a) and (5b) eliminates the singularity, and the resulting first-order differential equation scales exactly, thus showing that even at $T \equiv 0$,

$\Delta_0/\sqrt{Av_E} = \text{const}$, and $2\Delta_0/k_B T_c = \text{const}$. Numerically, we have found that the $T>0$ result extrapolates smoothly to the $T=0$ result, verifying our analytic analysis.

III. VERY-STRONG-COUPLING RESULTS

A. Zero temperature

In Fig. 1 we show results for (a) the real and imaginary components of the gap function $\Delta(\omega)$, (b) the real and imaginary components of the renormalization function $Z(\omega)$, (c) the spectral function at the Fermi level

$$A(k_F, \omega) = \frac{-1}{\pi} \text{Im} \left[\frac{\omega}{Z(\omega)[\omega^2 - \Delta^2(\omega)]} \right],$$

and (d) the quasiparticle density of states,

$$\frac{N(\omega)}{N(0)} = \text{Re} \left[\frac{\omega}{\sqrt{[\omega^2 - \Delta^2(\omega)]^{1/2}}} \right],$$

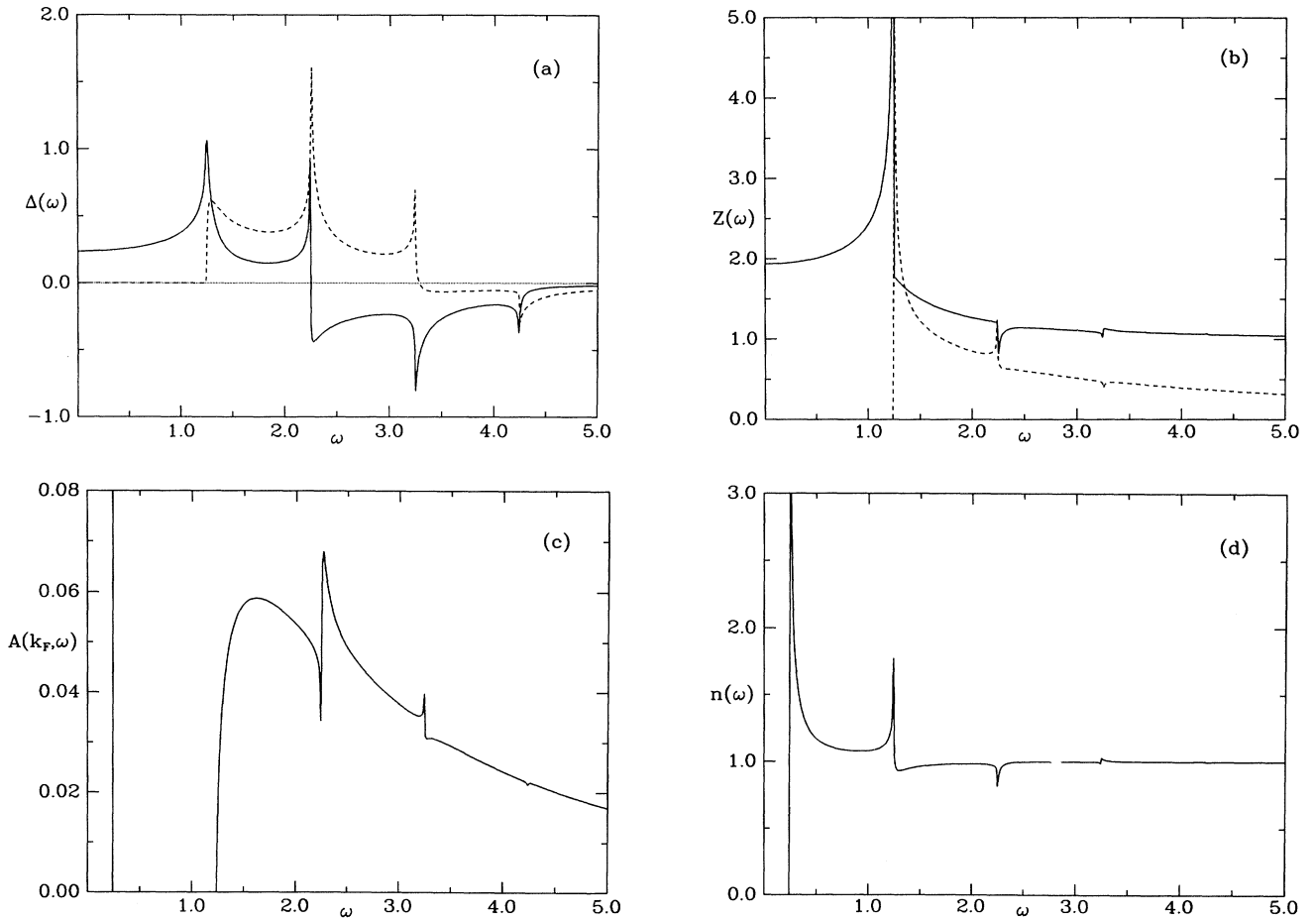


FIG. 1. Results for an Einstein boson spectral function with $\lambda=1.0$ and $v_E=1.0$ meV at $T=0$. In this and all subsequent figures the solid line refers to the real part and the dashed line (if present) refers to the imaginary part. All energy units in the figures are meV. We plot (a) the gap function $\Delta(\omega)$, (b) the renormalization function $Z(\omega)$, (c) the spectral function at the Fermi level, $A(k_F, \omega)$, and (d) the quasiparticle density of states normalized to the normal state, $n(\omega) \equiv N(\omega)/N(0)$. In all figures the gap and/or structure at frequencies $\omega = \Delta_0 + nv_E$, $n = 1, 2, 3, \dots$ are present. See text for detailed explanation.

as a function of frequency, for the case $\lambda=1$, $v_E=1.0$ meV, at zero temperature (actually, $T/T_c=0.1$, as discussed earlier). In all four figures there is structure occurring at energies $\omega=\Delta_0+nv_E$, $n=0,1,2,\dots$ due to multiple boson emissions. Here, Δ_0 is the gap edge, determined (for any temperature) by the condition

$$\Delta_0 = \text{Re}\Delta(\omega=\Delta_0), \quad (6)$$

which when fulfilled, gives rise to the singularity in the density of states. The spectral function shows a quasiparticle peak at the gap edge, followed by a “gap” equal to the boson frequency v_E , followed by the continuum. In Fig. 1(a) “resonances” occur in the real part of the gap function at both Δ_0+v_E and Δ_0+2v_E before the real part changes sign at $\omega=\Delta_0+2v_E$. The main resonance in the imaginary part of the gap also occurs at ω_0+2v_E . [For a Lorentzian shaped boson spectral function the change of sign of $\text{Re}\Delta(\omega)$ and the main resonance in $\text{Im}\Delta(\omega)$ both occur closer to $\omega=\Delta_0+v_E$.¹⁵] The important thing to note is that the structure occurs on the scale of the exchange boson, displaced from the Fermi level by the gap

Δ_0 , as was appreciated many years ago.¹⁵

We show the same four functions in Figs. 2(a)–2(d), now for the rather extreme case, $\lambda=100$, $v_E=0.02$ meV. Structure on the scale of v_E is readily observable in all four figures, again due to multiple boson emission processes. However, structure has also clearly developed on a completely different energy scale. In Fig. 2(c), for example, the quasiparticle peak occurs at the gap edge, $\Delta_0 \approx 0.19$ meV. The second pronounced resonance occurs at $\omega=0.57$, that is, at approximately $\omega=3\Delta_0$. We have verified that this is not accidental by checking $\lambda=50$ and $\lambda=200$. In all three cases the second resonance occurs at approximately $\omega=3\Delta_0$. Multiple peaks occur at higher energies, with frequencies of order Δ_0 apart. Some results concerning $\lambda=1, 50, 100$, and 200 are summarized in Table I. T_c clearly obeys the behavior $T_c \propto \sqrt{\lambda}v_E$ for the last three rows in Table I whereas Δ_0 does not quite. (Claims that $\Delta_0 \propto \lambda$ are, however, clearly incorrect.) The gap ratio, $2\Delta_0/k_B T_c$, therefore, has not saturated, but in any event appears to be following the behavior, $2\Delta_0/k_B T_c \sim c_0 - g(\lambda)$, where c_0 is the $\lambda \rightarrow \infty$ value for

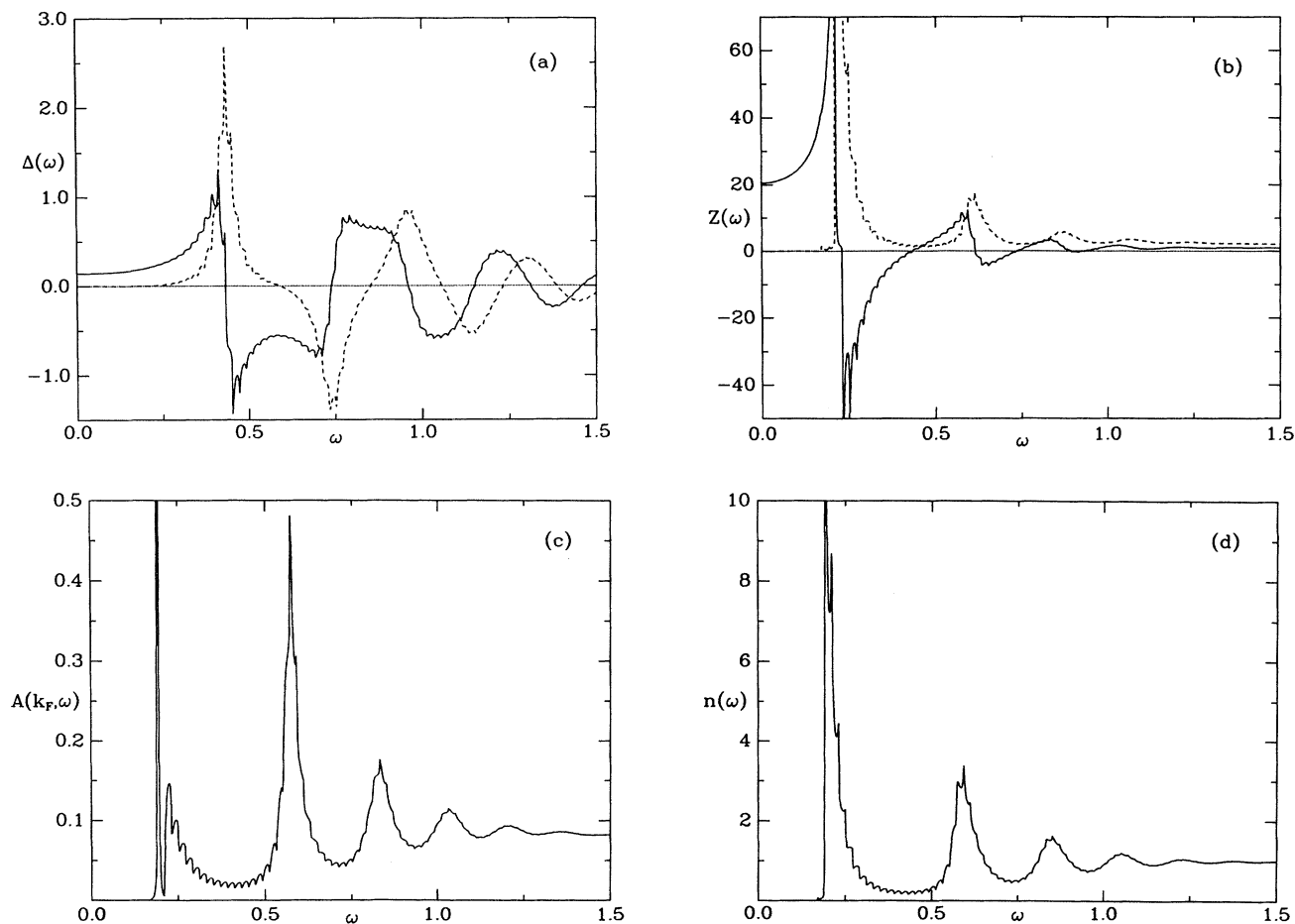


FIG. 2. Same legend as for Fig. 1 but for the very-strong-coupling regime. Here, $\lambda=100$, $v_E=0.02$ meV. The same type of structure as observed in Fig. 1 is present here. In addition, there are prominent oscillations on the scale of the gap edge Δ_0 presumably due to excitations involving additional broken Cooper pairs.

TABLE I. Summary of results for $\lambda=1, 50, 100,$ and 200 . The quantity ω_2 gives the frequency of the second peak apparent in, for example, Fig. 2(c) or Fig. 2(d).

λ	v_E (meV)	T_c (meV)	Δ_0 (meV)	$\frac{2\Delta_0}{k_B T_c}$	ω_2 (meV)
1	1.0	0.1146	0.242	4.23	
50	0.04	0.0513	0.254	9.92	0.81
100	0.02	0.0364	0.192	10.54	0.57
200	0.01	0.0258	0.142	11.04	0.41

the ratio and $g(\lambda) \rightarrow 0$ in that limit. We will return to the value of c_0 in Sec. IV.

Although we are apparently well outside the assumed validity of Eliashberg theory,¹⁷ it is tempting to interpret our results in terms of tightly bound pairs.¹⁸ Then, the spectral function has a resonance at $\omega=3\Delta_0$ corresponding to the process whereby an injected electron (energy $=\Delta_0$) breaks up a single Cooper pair (energy $=2\Delta_0$) for a total energy of the required amount. The higher-order peaks apparent in Fig. 2 are presumably due to higher-order effects contained in the nonlinearity of the

equations. The resonance need not occur at precisely $3\Delta_0$ since there is an intrinsic imaginary component in the self-energy. This is apparent in the gap function [Fig. 2(a)] and the renormalization function, $Z(\omega)$ [Fig. 2(b)]. There is a substantially increased amplitude for this process to occur in this limit because now the Cooper pairs are tightly bound and not spread over many other pairs as in the conventional regime. If this interpretation is correct it is indeed remarkable that Eliashberg theory gives a qualitative description at $T=0$ in the strong-coupling regime.

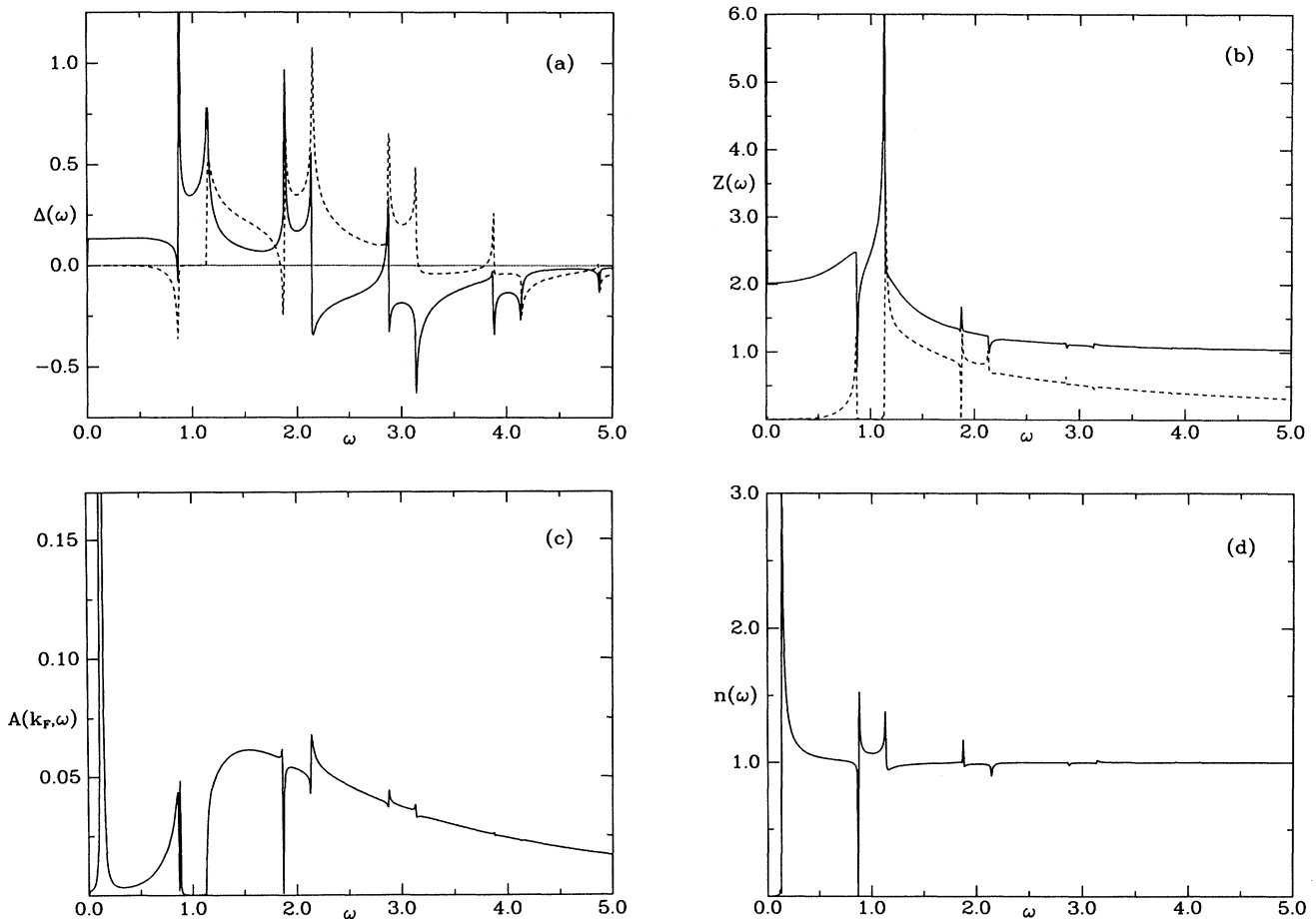


FIG. 3. Same as Fig. 1 except at $t \equiv T/T_c = 0.9$. See text for detailed explanation of structure.

B. Finite temperature

It is interesting to consider the case of finite temperature in this regime as well. Let us first review the conventional regime.¹⁵ In Figs. 3(a)–3(d) we plot $\Delta(\omega)$, $Z(\omega)$, $A(k_F, \omega)$, and $N(\omega)/N(0)$, respectively, for $\lambda=1.0$, $v_E=1.0$, and $t \equiv T/T_c=0.9$. Note that the structure remains sharp even at temperatures near T_c . A well-defined albeit reduced gap exists. This is simply due to the fact that $T_c/v_E \sim 0.1$, so that the Fermi and Bose functions are still very sharp. Structure again occurs at frequencies $\Delta_0(T=0.9T_c) + nv_E, n=0, 1, 2, \dots$ where now the displacement from the Fermi energy is given by the reduced finite-temperature gap edge. In addition, new resonances have appeared at frequencies $-\Delta_0(T=0.9T_c) + nv_E, n=1, 2, 3, \dots$. These are understood¹⁵ to arise from new decay channels available at finite temperature. Excited quasiparticles exist, particularly at $\omega = \Delta_0(t)$. There is an increased probability that an injected electron will recombine with this excited quasiparticle, through the emission of a phonon, resulting in a resonance occurring at the frequency $v_E - \Delta_0(t)$, as is

seen in the spectral function [Fig. 3(c)], for example. We should stress that both types of these resonances arise from phonon emission, that is, the terms involving $z - v_E$ in Eqs. (4) rather than those involving $z + v_E$. (Note that

$$N(v_E) + f(v_E - \omega) = \frac{[1 + N(v_E)][1 - f(\omega - v_E)]}{[1 - f(\omega)]}$$

and

$$N(v_E) + f(v_E + \omega) = N(v_E)[1 - f(v_E + \omega)]/[1 - f(\omega)]$$

(Ref. 19).) In fact, for the model displayed in Figs. 1 and 3 ($\lambda=1, v_E=1$) we can leave out the “ $\omega + v_E$ ” terms in Eqs. (4), and the results do not change. A conspicuous feature in Fig. 3(c) is a “gap” existing centered around $\omega = v_E$. This “gap” is a natural extension of the “gap” at $T=0$ [Fig. 1(c)]. There is no contribution above $\omega = v_E - \Delta_0$ because the recombination processes mentioned above are greatly suppressed due to a lack of excited quasiparticles with which to recombine. Spectral weight occurs again at $\omega = v_E + \Delta_0$, as at $T=0$, so that a “gap” $\approx 2\Delta_0(t)$ occurs centered around $v_E = 1.0$.

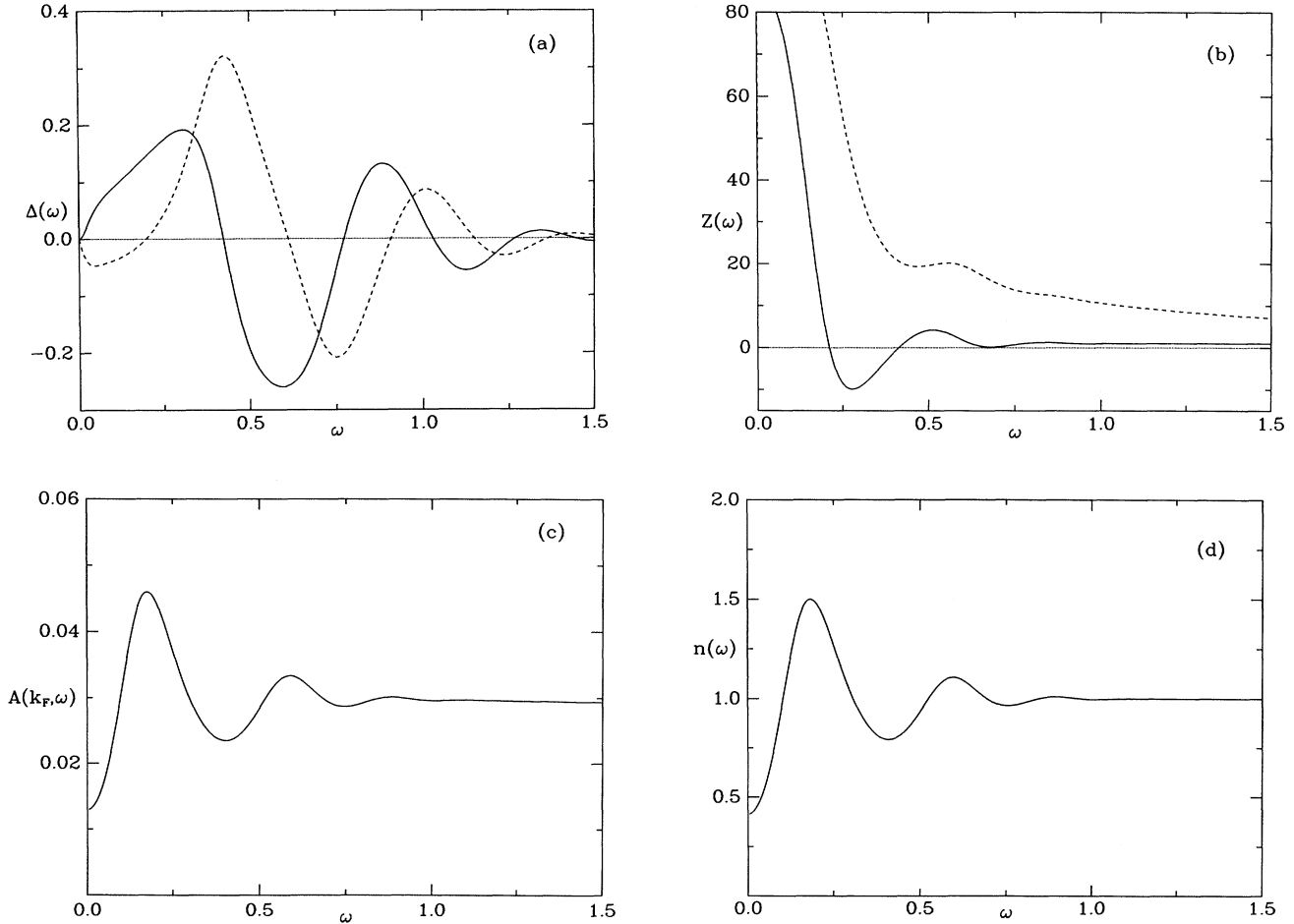


FIG. 4. Same as Fig. 2 except at $t \equiv T/T_c = 0.9$. Structure due to phonon scatterings has been thermally smeared. The oscillations remain, however, on the scale of the zero-temperature gap edge.

In Figs. 4(a)–4(d) we plot the corresponding results in the very-strong-coupling regime ($\lambda=100$, $v_E=0.02$ meV, $t=0.9$). Thermal smearing is now dominant, since T_c (as determined within Eliashberg theory²⁰) is greater than the boson frequency, v_E (Table I). Nonetheless, oscillations on the scale of the zero-temperature value of the gap, $\Delta_0(T=0)$, remain, even close to T_c . This is somewhat expected since the temperature at $T=0.9T_c$ is still much lower than the gap energy, $\Delta_0(T=0)$, which provided the energy scale for structure at $T=0$. Other minor differences occur. In Fig. 4(a), for example, the real part of the gap function goes to zero at the Fermi level, $\text{Re}\Delta(\omega) \propto \omega^2$, and the imaginary part is nonzero immediately off the Fermi level, with behavior $\text{Im}\Delta(\omega) \propto \omega$.²¹ Similarly, $\text{Im}Z(\omega)$ is very large at $\omega=0$ at finite temperature, whereas it is zero at $T=0$. (This was also the case in Fig. 2 though at extremely small frequency scales.) Also note that, according to Eq. (6), a gap is present at $t=0.9$, although the spectral function or density of states shows no true gap at $t=0.9$ (in contrast to the case for $\lambda=1$, $v_E=1.0$ at $t=0.9$).

The full temperature dependence of the gap edge is displayed in Fig. 5, for the weak-coupling BCS case, and for $\lambda=100$, $v_E=0.02$ meV. The moderately-strong-coupling case, $\lambda=1.0$, $v_E=1.0$ (not shown) deviates only slightly from the weak-coupling BCS result (larger values). The result in very strong coupling is first of all multivalued, a fact noted by Leavens.²² This behavior is an artifact of the definition of the gap edge given by Eq. (6). The true order parameter does indeed approach zero and is single valued as $T \rightarrow T_c$. The other noteworthy difference between the two cases illustrated in Fig. 5 is the temperature dependence as $T \rightarrow 0$. The BCS result shows a constant gap edge out to $t=0.3$, whereas in the

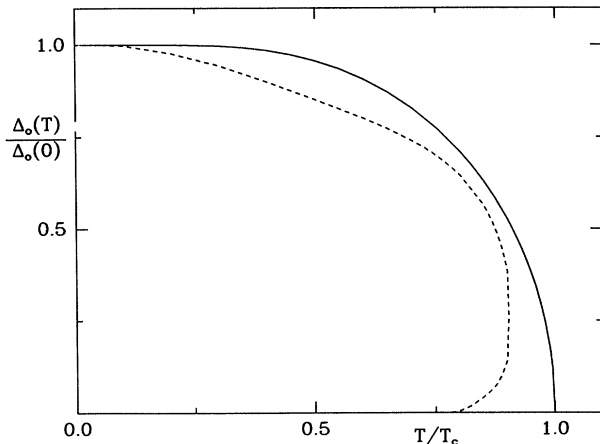


FIG. 5. Plot of the gap edge normalized to its zero-temperature value, $\Delta_0(T)/\Delta_0(0)$ vs T/T_c for a weak-coupling BCS superconductor (solid line), and a very-strongly-coupled ($\lambda=100$, $v_E=0.02$ meV) Eliashberg superconductor (dashed line). The gap edge is defined through $\Delta_0 = \text{Re}\Delta(\omega=\Delta_0)$. For the latter case the gap edge becomes double valued at higher temperatures, but loses its physical significance at the same time.

very-strong-coupling case deviations are visible already at $t=0.1$. In this latter case it almost looks as if the gap edge does not have exponential behavior, as $T \rightarrow 0$, though we have found that it always does, at sufficiently low temperature.

The results shown in Fig. 5 are somewhat misleading, however. In a tunneling measurement, for example, essentially the density of states is extracted, which is the quantity illustrated in part (d) of Figs. 1–4. The gap edge is roughly associated with the frequency at which the peak in the density of states occurs. Figures 2(d) and 4(d) show that for very strong coupling this peak occurs at the same energy, independent of temperature, so one would conclude that a temperature-independent gap edge has been observed, which *does not go to zero at T_c* , in contrast to the case in moderate coupling [Figs. 1(d) and 3(d)] or the behavior suggested by Fig. 5. In all cases, of course, the order parameter does go smoothly to zero at $T=T_c$.

IV. ASYMPTOTIC LIMIT

For completeness we present results for $\lambda \rightarrow \infty$. Equation (3) has been solved for progressively lower temperatures, until the gap values were no longer changing but more Matsubara frequencies were simply being filled in. A plot of $\bar{\Delta}(i\omega_n)$ versus $\bar{\omega}_n$ is shown in Fig. 6, for $t=0.01$ and $t=0.02$. The two results are practically indistinguishable, indicating that we have essentially solved the $T=0$ case. It was necessary to use such a low reduced temperature in this case, as was noted with regard to Fig. 5. The analytic continuation was obtained with Eqs. (5a) and (5b) using progressively smaller values of \bar{v}_E until the results converged. As noted earlier, we imposed $T=0$ or $T>0$ conditions on the Fermi and Bose functions, and found a smooth extrapolation from $T>0$ to $T=0$. The results for $T=0$ and $t=0.9$ are shown in Figs. 7(a) and

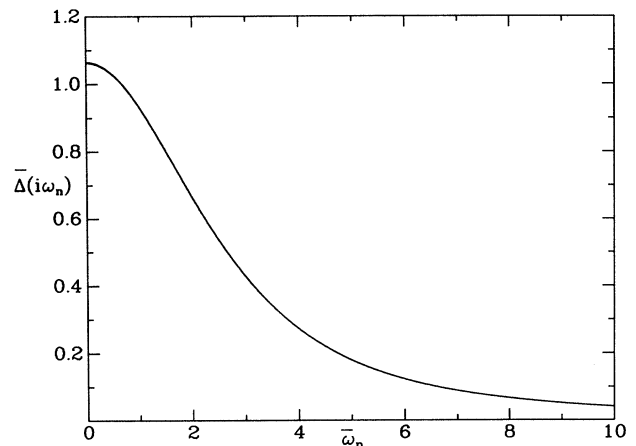


FIG. 6. Plot of the scaled gap function $\bar{\Delta}(i\omega_n)$ as a function of scaled Matsubara frequency $\bar{\omega}_n (Q \equiv Q/\sqrt{Av_E})$ at $t=0.01$ (solid) and $t=0.02$ (dotted), in the asymptotic limit. The two curves are barely discernible, indicating that we have solved for the “zero-temperature” gap function. The result is featureless except for a broad maximum at the origin.

7(b) and Figs. 8(a) and 8(b), respectively. As a check we solved a case with $\lambda=1000$ using the unscaled equations, and found essentially identical results except for extra noise due to the nonzero boson frequency.

Figure 7(a) shows the real and imaginary parts of the gap function with the oscillatory behavior noted earlier. All plots are in scaled units, e.g., $\bar{\omega} \equiv \omega/\sqrt{Av_E}$. The main resonance in $\text{Im}\bar{\Delta}(\omega)$ [along with the change of sign in $\text{Re}\bar{\Delta}(\omega)$] occurs at $2\bar{\Delta}_0$. $\text{Re}\bar{\Delta}(\omega)$ and $\bar{\omega}$ never actually cross; they become tangential at $\bar{\omega}=\bar{\Delta}_0$, with the result that $\partial\bar{\Delta}(\omega)/\partial\bar{\omega}|_{\bar{\omega}=\bar{\Delta}_0} \equiv 1$. In Fig. 7(b) the density of states clearly exhibits multiple resonances, starting with the main one at $\bar{\omega}=\bar{\Delta}_0$. At finite temperature the structure persists, and Fig. 8(b) shows the first two peaks in the

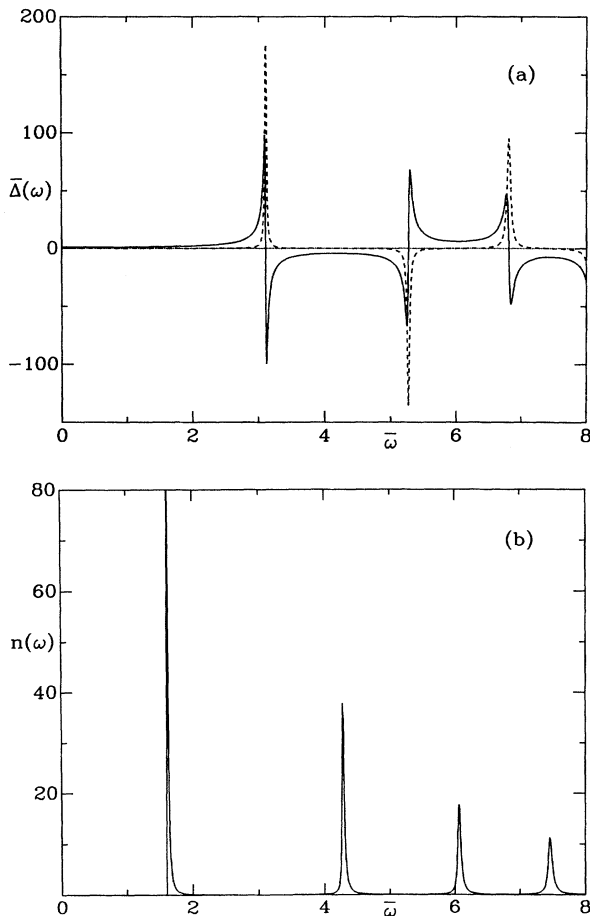


FIG. 7. Plot of (a) the scaled gap function $\bar{\Delta}(\omega)$ and (b) the density of states $n(\omega) \equiv N(\omega)/N(0)$, as a function of scaled (real) frequency $\bar{\omega}$ at zero temperature. The gap function is highly oscillatory on a scale of the gap edge Δ_0 . In (b) the gap edge is obvious. In (a) it is determined by drawing the line $g(\omega)=\bar{\omega}$ and finding the intersection with the real part of the gap function. These curves are actually tangential at $\bar{\omega} \sim 1.62$. The multiple peaks seen in (b) arise from the near tangency of the lines $g(\omega)=\pm\bar{\omega}$ with $\text{Re}\bar{\Delta}(\bar{\omega})$ in (a) at the various frequencies of the peaks in (a).

density of states at roughly the same frequency as at $T=0$.

At zero temperature we obtain an asymptotic value of the gap ratio, $2\Delta_0/k_B T_c = 12.7$. The asymptotic scaling, $T_c \propto v_E \sqrt{\lambda} \propto \sqrt{Av_E}$ occurs for relatively small λ (≈ 10). In contrast, the scaling behavior for the gap edge, $\Delta_0 \propto v_E \sqrt{\lambda} \propto \sqrt{Av_E}$ only arises for much higher values of λ . Kresin⁷ has used an approximate analysis and arrived at an asymptotic value for $2\Delta_0/k_B T_c$ similar to ours. However, his form for the gap function does not appear to be correct. Figures 6 and 7 suggest a form:

$$\Delta(i\omega_n) \approx f(i\omega_n) \text{sech} \left[\frac{\omega_n}{g(i\omega_n)} \right],$$

where $f(i\omega_n)$ and $g(i\omega_n)$ are slowly varying functions of ω_n , of energy scale, Δ_0 . This form fits the result in Fig. 6 very well. Upon analytic continuation,

$$\Delta(\omega+i\delta) \approx f(\omega) \text{sec} \left[\frac{\omega}{g(\omega)} \right],$$

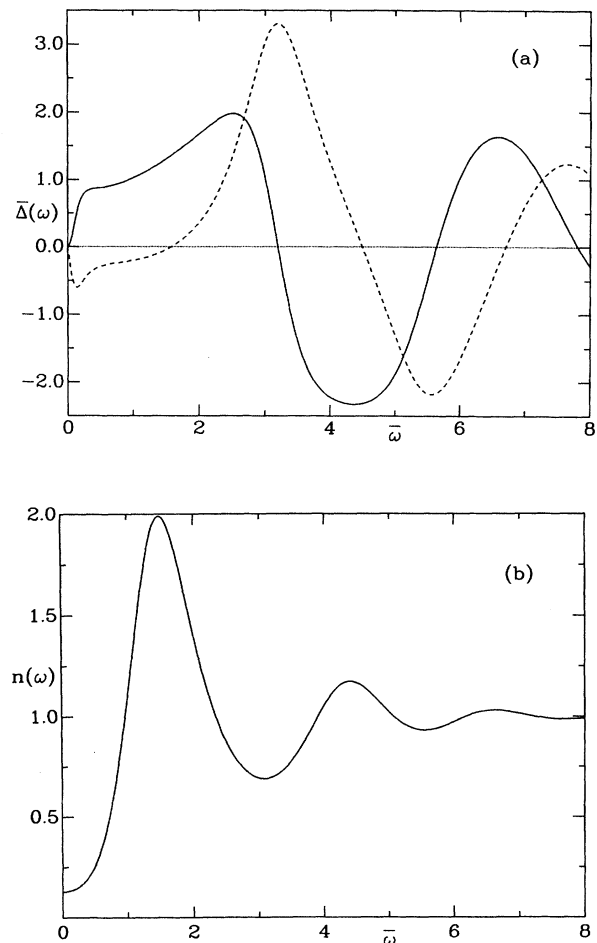


FIG. 8. Same as in Fig. 7, except for $t=0.9$. The two most prominent peaks in (b) occur at nearly the same frequency as in Fig. 7(b).

so that the oscillations characteristic of $\sec x$ become prominent, as is the case in Fig. 7.

The renormalization function and spectral function are given by simple expressions, at $T=0$, in the asymptotic limit. From Eq. (5b) it readily follows that

$$Z(\bar{\omega}) = 1 + \frac{i\pi}{\bar{v}_E} \frac{1}{[\bar{\omega}^2 - \bar{\Delta}^2(\bar{\omega})]^{1/2}} \quad (7)$$

with the second term of course dominating as $\bar{v}_E \rightarrow 0$. The spectral function at the Fermi level then becomes

$$A(k_F, \omega) = \frac{A}{\pi^2} \frac{N(\omega)}{N(0)}, \quad (8)$$

where $A = (\lambda v_E / 2)$ is the area in the boson spectral function. Equation (8) is seen to be already obeyed on comparison of Figs. 2(c) and 2(d), for example.

V. CONCLUSIONS

We have calculated the Eliashberg gap and renormalization functions in the very-strong-coupling ($\lambda \gg 1$) and asymptotic ($\lambda \rightarrow \infty$) regimes, for a gas of electrons interacting with Einstein bosons of frequency v_E . In the

conventional regime ($\lambda \sim 1$) these functions, along with the derived spectral function and density of states, exhibit a gap followed by an incoherent part which contains structure due to boson emission. By contrast, in the unconventional regime investigated in this paper, structure becomes prominent on the scale of the gap edge energy, Δ_0 . This added structure appears to be due to excitations involving broken Cooper pairs, due to the substantially decreased coherence length in this limit. This implies that at zero temperature, Eliashberg theory qualitatively describes the limit of tightly bound Cooper pairs, provided other instabilities are avoided. This asymptotic behavior persists for much more moderate values of the mass enhancement λ than considered in this paper, and may be realizable in physical systems.

ACKNOWLEDGMENTS

This research received partial financial support from the Natural Sciences and Engineering Research Council of Canada (NSERC), from National Science Foundation (NSF) Grant No. DMR-8918306 (F.M.), and from the Canadian Institute for Advanced Research (CIAR) (J.P.C.).

*Present address: Theoretical Physics Branch, AECL, Chalk River Laboratory, Chalk River, Ontario, Canada K0J 1J0.

¹See, for example, Proceedings of the International Conference on Materials and Mechanisms of Superconductivity High Temperature Superconductors II, Stanford University, CA, 1989, edited by R. N. Shelton, W. A. Harrison, and N. E. Phillips [Physica C **162-164** (1989)].

²See, for example, M. Tachiki and S. Takahashi, Phys. Rev. B **39**, 293 (1989); J. Friedel, J. Phys. Condens. Matter **1**, 7757 (1989).

³J. P. Carbotte, F. Marsiglio, and B. Mitrović, Phys. Rev. B **33**, 6135 (1986).

⁴L. N. Bulaevsii and O. V. Dolgov, Pis'ma Zh. Eksp. Teor. Fiz. **45**, 413 (1987) [JETP Lett. **45**, 526 (1987)].

⁵L. N. Bulzevsii, O. V. Dolgov, and M. O. Ptitsqn, Phys. Rev. B **38**, 11 290 (1988).

⁶O. V. Dolgov and A. A. Golubov, Int. J. Mod. Phys. B **1**, 1089 (1988).

⁷V. Z. Kresin, Solid State Commun. **63**, 725 (1987).

⁸F. Marsiglio, P. J. Williams, and J. P. Carbotte, Phys. Rev. B **39**, 9595 (1989); F. Marsiglio, J. P. Carbotte, and P. J. Williams, *ibid.* **41**, 4484 (1990); F. Marsiglio and J. P. Carbotte, *ibid.* **41**, 11 114 (1990).

⁹J. P. Carbotte and F. Marsiglio, in *Studies of High Temperature Superconductors*, edited by A. V. Narlikar (Nova Science Publishers, New York, 1989), Vol. 1, p. 64.

¹⁰P. B. Allen and R. C. Dynes, Phys. Rev. B **12**, 905 (1975).

¹¹C. S. Owen and D. J. Scalapino, Physica **55**, 691 (1971).

¹²D. Rainer and G. Bergmann, J. Low Temp. Phys. **14**, 501

(1974).

¹³J. M. Daams and J. P. Carbotte, J. Low Temp. Phys. **43**, 263 (1981).

¹⁴F. Marsiglio, M. Schossmann, and J. P. Carbotte, Phys. Rev. B **37**, 4965 (1988).

¹⁵D. J. Scalapino, in *Superconductivity*, edited by R. D. Parks (Marcel Dekker, New York, 1969), Vol. 1, p. 449.

¹⁶H. J. Vidberg and J. W. Serene, J. Low Temp. Phys. **29**, 179 (1977).

¹⁷See, however, F. Marsiglio [Physica C **162-164**, 1453 (1989) and Phys. Rev. B **42**, 2416 (1990)], for a quantum Monte Carlo study which suggests Eliashberg theory is accurate beyond the conditions of Migdal's approximation so long as other instabilities are avoided (as is assumed here). See also, R. T. Scalettar, N. E. Bickers, and D. J. Scalapino, Phys. Rev. B **40**, 197 (1989).

¹⁸This was first suggested to us by S. Kivelson (private communication).

¹⁹S. B. Kaplan, C. C. Chi, D. N. Langenberg, J. J. Chang, S. Jafarey, and D. J. Scalapino, Phys. Rev. B **14**, 4854 (1976).

²⁰In the very-strong-coupling limit T_c is presumably due to Boson "decondensation." Here T_c refers to the calculated Eliashberg value, due to pair dissociation, which will be different.

²¹A. E. Karakosov, E. G. Maksimov, and S. A. Mashkov, Zh. Eksp. Teor. Fiz. **68**, 1937 (1957); Sov. Phys. JETP **41**, 971 (1976).

²²C. R. Leavens, Phys. Rev. B **29**, 5178 (1984).